Cosmic Microwave Background Constraints Cast a Shadow On Continuous Spontaneous Localization Models

Jérôme Martin[1,*] and Vincent Vennin[2,1,†]
[1]Institut d'Astrophysique de Paris, UMR 7095-CNRS, Université Pierre et Marie Curie, 98bis boulevard Arago, 75014 Paris, France
[2]Laboratoire Astroparticule et Cosmologie, Université Denis Diderot Paris 7, 75013 Paris, France

(Received 22 June 2019; accepted 26 November 2019; published 26 February 2020)

The continuous spontaneous localization model solves the measurement problem of standard quantum mechanics by coupling the mass density of a quantum system to a white-noise field. Since the mass density is not uniquely defined in general relativity, this model is ambiguous when applied to cosmology. We however show that most natural choices of the density contrast already make current measurements of the cosmic microwave background incompatible with other laboratory experiments.

DOI: 10.1103/PhysRevLett.124.080402

Addressing the measurement (or macro-objectification) problem is a central issue in quantum mechanics, and three classes of solutions have been put forward [1]. One can either (1) leave quantum theory unmodified and consider different interpretations (e.g., Copenhagen, many worlds, Qbism, etc.), (2) extend the mathematical framework and introduce additional degrees of freedom (e.g., de Broglie-Bohm), or (3) consider that quantum theory is an approximation of a more general framework and that, outside its domain of validity, it differs from the standard formulation. Dynamical collapse models [1–5] follow this last reasoning and introduce a nonlinear and stochastic modification to the Schrödinger equation. Remarkably, the structure of this modification is essentially unique. Through an embedded amplification mechanism, this allows microscopic systems to be described by the standard rules of quantum mechanics while preventing macroscopic systems from being in a superposition of macroscopically distinct configurations. It also allows the Born rule to be derived rather than postulated [5]. Because they lead to predictions that are different from that of conventional quantum mechanics, dynamical collapse models are falsifiable contrary to the other options mentioned before (except de Broglie-Bohm theory in the out-of-equilibrium regime [6,7]).

Different versions of dynamical collapse theories correspond to different choices for the collapse operator (energy, momentum, spin, position), the nature of the stochastic noise (white or nonwhite), and whether dissipative effects are included or not. Only a collapse operator related to position can ensure proper localization in space, and three iconic theories have been proposed: (1) the Ghirardi-Rimini-Weber (GRW) model, which is historically the first one but is not formulated in terms of a continuous stochastic differential equation, (2) quantum mechanics with universal position localization, where the collapse operator is position but where the stochastic noise depends on time only, and (3) the continuous spontaneous localization (CSL) model [4], where the stochastic noise depends on time and space and where the collapse operator is the mass density. This version is the most refined of all three and features the modified Schrödinger equation

$$d|\Psi\rangle = \left\{-i\hat{H}dt + \frac{\sqrt{\gamma}}{m_0}\int d\boldsymbol{x}_p[\hat{\rho}_{\rm sm}(\boldsymbol{x}_p) - \langle\hat{\rho}_{\rm sm}(\boldsymbol{x}_p)\rangle]dW_t(\boldsymbol{x}_p) - \frac{\gamma}{2m_0^2}\int d\boldsymbol{x}_p[\hat{\rho}_{\rm sm}(\boldsymbol{x}_p) - \langle\hat{\rho}_{\rm sm}(\boldsymbol{x}_p)\rangle]^2 dt\right\}|\Psi\rangle, \tag{1}$$

where $\hat{H}$ is the standard Hamiltonian of the system, $\langle\hat{A}\rangle \equiv \langle\Psi|\hat{A}|\Psi\rangle$, γ is the first free parameter of the theory, m_0 is a reference mass (usually the mass of a nucleon), $W_t(\boldsymbol{x}_p)$ is an ensemble of independent Wiener processes (one for each point in space), and $\hat{\rho}_{\rm sm}$ is the smeared mass density operator,

$$\hat{\rho}_{\rm sm}(\boldsymbol{x}_p) = \frac{1}{(2\pi)^{3/2}{r_c}^3}\int d\boldsymbol{y}_p\hat{\rho}(\boldsymbol{x}_p + \boldsymbol{y}_p)e^{-|\boldsymbol{y}_p|^2/2r_c^2}, \tag{2}$$

where r_c is the second free parameter of the theory. The two parameters γ and r_c have been constrained in various laboratory experiments. The strongest bounds so far come from x-ray spontaneous emission [8], force noise measurements on ultracold cantilevers [9], and gravitational-wave interferometers [10]. These constraints leave the region of parameter space around $r_c \sim 10^{-8}$–10^{-4} m and $\lambda \sim 10^{-18}$–10^{-10} s^{-1} viable, where $\lambda \equiv \gamma/(8\pi^{3/2}r_c^3)$, corresponding to the white region in Fig. 3.

Dynamical collapse models can also be constrained in a cosmological context [11–18]. Indeed, the typical physical scales involved in cosmology are many orders of magnitude different from those encountered in the laboratory and this may lead to competitive constraints (in the early Universe, energy scales can be as high as $\sim 10^{15}$ GeV, corresponding to densities of $\sim 10^{80}$ $g \times {\rm cm}^{-3}$). Moreover, one can argue that the quantum measurement problem (as well as the quantum-to-classical transition issue [19–22]) is even more acute in cosmology than in the laboratory [23] due to the difficulties in introducing an "observer" as in the standard Copenhagen interpretation [24,25].

Although the quantum state of cosmological perturbations, $|\Psi_{2\mathrm{sq}}\rangle$, is a two-mode squeezed state that features some classical properties [20,26,27], it is not an eigenstate of the cosmic microwave background (CMB) temperature anisotropies, so how the process

$$|\Psi_{2\,\mathrm{sq}}\rangle = \sum c(\ )|\ \rangle \to |\ \rangle_{\mathrm{Planck}} \tag{3}$$

occurred is unclear. This makes the early Universe a perfect arena to test CSL.

The leading paradigm to describe this epoch is cosmic inflation [28–32], which was introduced in order to solve the puzzles of the standard hot Big-Bang phase. Inflation is believed to have been driven by a scalar field ϕ, named the "inflaton," the physical nature of which is still unknown, although detailed constraints on the shape of its potential now exist [33–41]. Inflation also provides a convincing mechanism for structure formation according to which galaxies and CMB anisotropies are nothing but quantum vacuum fluctuations amplified by gravitational instability and stretched to astrophysical scales [42]. This mechanism fits very well the high-accuracy astrophysical data now at our disposal, in particular the CMB temperature and polarization anisotropies [43,44].

The Universe is well described by a flat, homogeneous, and isotropic metric of the Friedmann-Lemaître-Robertson-Walker (FLRW) type, $ds^2 = -dt^2 + a^2(t)\delta_{ij}dx^i dx^j$, where x^i is the comoving spatial coordinate, t refers to cosmic time, and $a(t)$ is the scale factor which depends on time only. During inflation, the expansion is accelerated, $\ddot{a} > 0$, and the Hubble parameter $H = \dot{a}/a$ (where a dot denotes derivation with respect to time) is almost constant; see Fig. 1.

To describe the small quantum fluctuations living on top of this FLRW background, the metric and inflaton fields are expanded according to $g_{\mu\nu} = g_{\mu\nu}^{\mathrm{FLRW}}(t) + \delta\hat{g}_{\mu\nu}(t,\boldsymbol{x})$ and $\phi = \phi^{\mathrm{FLRW}}(t) + \delta\hat{\phi}(t,\boldsymbol{x})$ with $|\delta g_{\mu\nu}/g_{\mu\nu}^{\mathrm{FLRW}}| \ll 1$ and $|\delta\phi/\phi^{\mathrm{FLRW}}| \ll 1$. This gives rise to two types of perturbations, scalars and tensors. Tensors correspond to primordial gravitational waves and have not yet been detected, the tensor-to-scalar ratio r being $r \lesssim 0.064$ [44]. Then, scalar perturbations can be described with a single gauge-invariant degree of freedom, the so-called curvature perturbation $\hat{\zeta}(t,\boldsymbol{x})$ [42,45], which can be directly related to temperature anisotropies. Expanding the action of the system (namely the Einstein-Hilbert action plus the action of a scalar field) up to second order in the perturbations leads to the Hamiltonian of the perturbations, $\hat{H} = \int_{\mathbb{R}^{3+}} d^3\boldsymbol{k}[\hat{p}_{\boldsymbol{k}}^2 + \omega^2(k,\eta)\hat{v}_{\boldsymbol{k}}^2]$, where $\hat{v}_{\boldsymbol{k}} \equiv z\hat{\zeta}_{\boldsymbol{k}}$ is the Mukhanov-Sasaki variable. One has introduced $z \equiv a\sqrt{2\epsilon_1}M_{\mathrm{Pl}}/c_S$ where c_S is the speed of sound ($c_S = 1$ for a scalar field) and $\epsilon_1 \equiv -\dot{H}/H^2$ is the first Hubble-flow parameter [46,47]. In the above expressions, the curvature perturbation has been Fourier transformed, $\hat{\zeta}(\eta,\boldsymbol{x}) = (2\pi)^{-3/2}\int d^3\boldsymbol{k}\hat{\zeta}_{\boldsymbol{k}}(\eta)e^{i\boldsymbol{k}\cdot\boldsymbol{x}}$, as appropriate for a linear theory where the modes evolve independently [48]. The conjugate momentum is $\hat{p}_{\boldsymbol{k}} \equiv \hat{v}_{\boldsymbol{k}}{}'$, where a prime denotes derivation with respect to the conformal time η defined via $dt = ad\eta$. Each mode behaves as a parametric oscillator, $\hat{v}_{\boldsymbol{k}}{}'' + \omega^2(k,\eta)\hat{v}_{\boldsymbol{k}} = 0$, with a time-dependent frequency $\omega^2(k,\eta) = c_S^2 k^2 - z''/z$ that involves the background dynamics. This phenomenon, described by the interaction between a quantum field (here the cosmological perturbations) and a time-dependent classical source (here the background spacetime), leads to parametric amplification and can be found in many other branches of Physics (e.g., the Schwinger effect [49], the dynamical Casimir effect [50], Unruh [51], and Hawking [52] effects, etc.).

Quantization of parametric oscillators yields squeezed states, which are Gaussian states. Solving the Schrödinger equation with the above Hamiltonian leads to $\Psi[v] = \prod_{\boldsymbol{k},s}\Psi_{\boldsymbol{k}}^s(v_{\boldsymbol{k}}^s)$, where $s = R,I$ labels the real and imaginary parts of $v_{\boldsymbol{k}}$, with $\Psi_{\boldsymbol{k}}^s(v_{\boldsymbol{k}}^s) = N_{\boldsymbol{k}}e^{-\Omega_k(v_{\boldsymbol{k}}^s)^2}$,

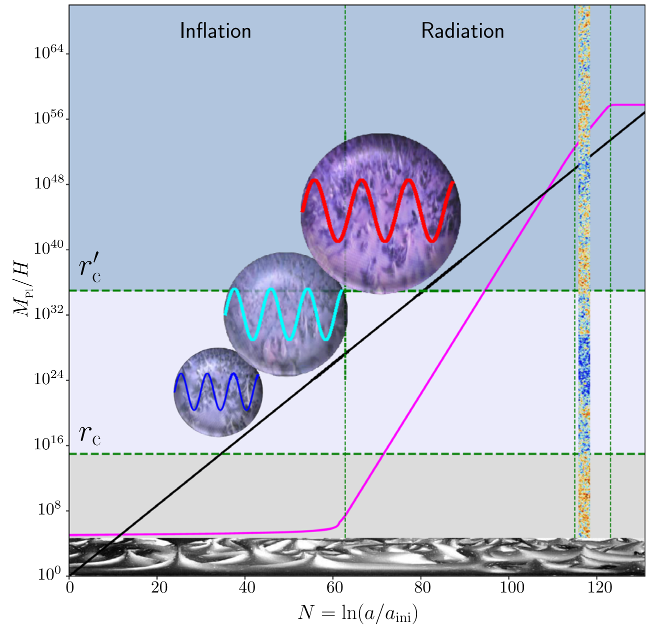

FIG. 1. Time evolution of the physical distances at play in the early Universe. During inflation, the Hubble radius H^{-1} (magenta line) is almost constant and, due to the expansion, the wavelength λ_k of a Fourier mode (black line) for a given quantum field crosses out that scale, above which spacetime curvature sources parametric amplification. In the subsequent Universe, H^{-1} increases faster than the scale factor a; hence, λ_k crosses the Hubble radius back in. Depending on the value of r_c, λ_k may cross out r_c either during inflation (r_c) or during the radiation era (r'_c).

$|N_{\boldsymbol{k}}| = (2\Re\mathrm{e}\Omega_{\boldsymbol{k}}/\pi)^{1/4}$, and $\Omega_{\boldsymbol{k}}$ obeying the equation $\Omega_{\boldsymbol{k}}{}' = -2i\Omega_{\boldsymbol{k}}^2 + i\omega^2(k,\eta)/2$. In the standard approach, $\langle \hat{v}_{\boldsymbol{k}} \rangle = 0$ and one needs to assume the existence of a specific process (3) that led to a particular realization corresponding to our Universe (this is the macro-objectification problem mentioned above). The dispersion of the different realizations is characterized by the two-point correlation function $\langle \zeta^2 \rangle = \int \mathcal{P}_\zeta d\ln k$ where $\mathcal{P}_\zeta = k^3|\zeta_{\boldsymbol{k}}|^2/(2\pi^2)$ is the power spectrum, which is predicted to be of the form $A_S k^{n_S-1}$ where n_S should be close to one. The recent Planck data (identifying spatial and ensemble averages) have confirmed this result with $\ln(10^{10}A_S) = 3.044 \pm 0.014$ and $n_S = 0.9649 \pm 0.0042$ [44].

If quantum theory is described by CSL rather than by the standard framework, the behavior of the cosmological perturbations is modified according to Eq. (1). In that case, the mass density is given by $\rho = \bar{\rho} + \delta\rho$, where $\bar{\rho}$ is the homogeneous component of the energy density satisfying the Friedmann equation $\bar{\rho} = 3M_{\mathrm{Pl}}^2 H^2$, M_{Pl} is the reduced Planck mass, and $\delta\rho$ the density fluctuation.

In general relativity (GR), however, there is no unique definition of the density contrast $\delta\rho/\bar{\rho}$. While all possible choices coincide on sub-Hubble scales where observations are performed, they can differ on super-Hubble scales. This introduces a fundamental ambiguity when defining CSL in cosmology: each choice for the density contrast leads to a different CSL theory. In order to illustrate how the calculation proceeds in details, we first consider the physically well-motivated choice consisting in measuring the energy density relative to the hypersurface which is as close as possible to a "Newtonian" time slicing (denoted δ_g in Ref. [53]). This leads to $\delta\rho/\bar{\rho} = \epsilon_1\zeta - \epsilon_1(1 + \epsilon_1 a^2 H^2 \partial^{-2})\zeta'/(3aH)$ if the Universe is dominated by a scalar field. Our aim is certainly not to argue in favor of that specific choice, and at the end of the Letter we generalize our results to an arbitrary definition of the density contrast.

From the previous considerations, Eq. (1) can be written in Fourier space as a set of independent CSL equations for the real and imaginary parts of each Fourier mode, in which the smeared mass density operator reads $\widehat{\delta\rho}^s_{\mathrm{sm}}(\boldsymbol{k}) = \alpha_{\boldsymbol{k}} \hat{v}^s_{\boldsymbol{k}} + \beta_{\boldsymbol{k}} \hat{p}^s_{\boldsymbol{k}}$ with

$$\alpha_{\boldsymbol{k}} \equiv \frac{M_{\mathrm{Pl}}^2 H^2 \epsilon_1}{z} e^{-k^2 r_c^2/2a^2} \left[4 + \frac{\epsilon_2}{2} - 3\left(\frac{aH}{k}\right)^2 \epsilon_1(1+\epsilon_2)\right], \tag{4}$$

$$\beta_{\boldsymbol{k}} \equiv \frac{M_{\mathrm{Pl}}^2 H \epsilon_1}{az} e^{-k^2 r_c^2/2a^2} \left[3\epsilon_1 \left(\frac{aH}{k}\right)^2 - 1\right], \tag{5}$$

where $\epsilon_2 \equiv d\ln\epsilon_1/d\ln a$ denotes the second Hubble-flow parameter. Because of the presence of the exponential term, the effect of the CSL terms is triggered only once the mode k under consideration crosses out the scale r_c, i.e., when its physical wavelength is larger than r_c, $k/a < r_c^{-1}$. Depending on the value of r_c, this can happen either during inflation or subsequently; see Fig. 1 (cases labeled r_c and r_c', respectively). Physically, it is clear that the CSL terms cannot "localize" a mode if its "size" (its wavelength) is smaller than the localization scale r_c. This also means that, at early time, when $k/a < r_c^{-1}$, the standard theory applies, which implies that one of the great advantages of inflation, namely the possibility to choose well-defined initial conditions in the Minkowski limit (the so-called Bunch-Davies vacuum state [54]), is preserved.

We are now in a position to solve Eq. (1). The most general stochastic Gaussian wave function can be written as

$$\Psi^s_{\boldsymbol{k}}(v^s_{\boldsymbol{k}}) = |N_{\boldsymbol{k}}(\eta)| \exp\{-\Re\mathrm{e}\Omega_{\boldsymbol{k}}(\eta)[v^s_{\boldsymbol{k}} - \bar{v}^s_{\boldsymbol{k}}(\eta)]^2 + i\sigma^s_{\boldsymbol{k}}(\eta) + i\chi^s_{\boldsymbol{k}}(\eta) v^s_{\boldsymbol{k}} - i\Im\mathrm{m}\Omega_{\boldsymbol{k}}(\eta)(v^s_{\boldsymbol{k}})^2\}, \tag{6}$$

where the free functions $\Omega_{\boldsymbol{k}}$, $\bar{v}^s_{\boldsymbol{k}}$, $\sigma^s_{\boldsymbol{k}}$, and $\chi^s_{\boldsymbol{k}}$ are (*a priori*) stochastic quantities. This wave packet is centered around $\langle \hat{v}^s_{\boldsymbol{k}} \rangle = \bar{v}^s_{\boldsymbol{k}}$ with a variance $\langle (\hat{v}^s_{\boldsymbol{k}} - \bar{v}^s_{\boldsymbol{k}})^2 \rangle = (4\Re\mathrm{e}\Omega_{\boldsymbol{k}})^{-1}$. The collapse of the wave function happens if the width of $\Psi(v^s_{\boldsymbol{k}})$ is much smaller than the typical dispersion of its mean, i.e.,

$$R \equiv \frac{\mathbb{E}[\langle (\hat{v}^s_{\boldsymbol{k}} - \bar{v}^s_{\boldsymbol{k}})^2 \rangle]}{\mathbb{E}(\bar{v}^{s2}_{\boldsymbol{k}})} \ll 1, \tag{7}$$

where $\mathbb{E}$ denotes the stochastic average. In fact, if the collapse occurs according to the Born rule, then $\mathbb{E}(\bar{v}^{s2}_{\boldsymbol{k}}) = \langle \hat{v}^{s2}_{\boldsymbol{k}} \rangle_{\gamma=0} = (4\Re\mathrm{e}\Omega_{\boldsymbol{k}}|_{\gamma=0})^{-1}$, and R can also be defined as $R = \mathbb{E}[\langle (\hat{v}^s_{\boldsymbol{k}} - \bar{v}^s_{\boldsymbol{k}})^2 \rangle]/\langle \hat{v}^{s2}_{\boldsymbol{k}} \rangle_{\gamma=0}$.

When the wave function has collapsed, its realizations are described by $\bar{v}^s_{\boldsymbol{k}}$. The power spectrum of the Mukhanov-Sasaki variable (or of curvature perturbation) is thus given by the dispersion of that quantity,

$$\mathcal{P}_v(k) = \frac{k^3}{2\pi^2}\{\mathbb{E}(\bar{v}^{s2}_{\boldsymbol{k}}) - [\mathbb{E}(\bar{v}^s_{\boldsymbol{k}})]^2\}. \tag{8}$$

The above quantity can also be rewritten as $\mathcal{P}_v(k) = k^3\{\mathbb{E}(\langle \hat{v}^{s2}_{\boldsymbol{k}} \rangle) - \mathbb{E}[\langle (\hat{v}^s_{\boldsymbol{k}} - \bar{v}^s_{\boldsymbol{k}})^2 \rangle]\}/(2\pi^2)$.

In order to calculate the quantities (7) and (8), one can insert the stochastic wave function (6) into Eq. (1) and solve the obtained stochastic differential equations. One obtains that $\Omega_{\boldsymbol{k}}$ decouples from the other free functions and obeys $\Omega'_{\boldsymbol{k}} = 4i\gamma a^4 \alpha_{\boldsymbol{k}} \beta_{\boldsymbol{k}} \Omega_{\boldsymbol{k}}/m_0^2 - 2(i + 2\gamma a^4 \beta_{\boldsymbol{k}}^2/m_0^2)\Omega_{\boldsymbol{k}}^2 + \gamma a^4 \alpha_{\boldsymbol{k}}^2/m_0^2 + i\omega^2(k,\eta)/2$. This equation is nonstochastic, as in the standard case, but contains new terms proportional to γ. Since it is nonstochastic, $\mathbb{E}[\langle (\hat{v}^s_{\boldsymbol{k}} - \bar{v}^s_{\boldsymbol{k}})^2 \rangle] = (4\Re\mathrm{e}\Omega_{\boldsymbol{k}})^{-1}$ and this implies that $R = \Re\mathrm{e}\Omega_{\boldsymbol{k}}|_{\gamma=0}/\Re\mathrm{e}\Omega_{\boldsymbol{k}}$.

In order to obtain the spectrum (8), $\mathbb{E}(\langle \hat{v}^{s2}_{\boldsymbol{k}} \rangle)$ remains to be determined. This is done by noticing that Eq. (1) can be cast into a Lindblad equation [55] for the averaged density matrix $\hat{\rho} = \mathbb{E}(|\Psi\rangle\langle\Psi|)$ [5]. From this Lindblad equation, one can derive a third-order differential equation for $\mathbb{E}(\langle \hat{v}^{s2}_{\boldsymbol{k}} \rangle)$ that can be solved exactly [56]. Combining the above mentioned results, one obtains

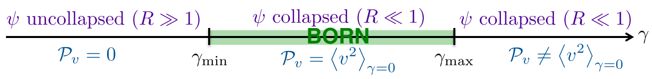

FIG. 2. Relevant values for γ. If $\gamma < \gamma_{\min}$, the wave function does not collapse and the power spectrum vanishes. If $\gamma > \gamma_{\max}$, the wave function collapses but the Born rule is violated and a non–scale-invariant power spectrum is obtained, which is excluded by the CMB observations. The region where $\gamma_{\min} < \gamma < \gamma_{\max}$, unbarred in Fig. 3, is where the wave function collapses to a scale-invariant power spectrum.

$$\mathcal{P}_v(k) \simeq \frac{k^3}{2\pi^2} \frac{1}{4\Re\mathrm{e}\Omega_{\boldsymbol{k}}|_{\gamma=0}} \left[1 + \frac{3}{2}\frac{\gamma}{m_0^2}\epsilon_1^3 \bar{\rho}_{\mathrm{inf}} \left(\frac{k}{aH}\right)^{-1}_{\mathrm{end}} - \frac{\Re\mathrm{e}\Omega_{\boldsymbol{k}}|_{\gamma=0}}{\Re\mathrm{e}\Omega_{\boldsymbol{k}}}\right], \tag{9}$$

where $\bar{\rho}_{\mathrm{inf}} = 3H_{\mathrm{inf}}^2 M_{\mathrm{Pl}}^2$ is the energy density during inflation. Depending on the value of γ, different results can be obtained, that are sketched in Fig. 2. If $\gamma = 0$, the state remains homogeneous and isotropic, and the spectrum vanishes. Then, when γ increases above a certain threshold, collapse occurs ($R \ll 1$), so the third term in Eq. (9) can be neglected. Provided the second term remains also negligible, the Born rule is thus recovered, and a scale-invariant power spectrum is obtained, in agreement with observations. Finally, when γ continues to increase so as to make the second term large, the power spectrum is no longer frozen on large scales and acquires a spectral index $n_S = 0$, which is excluded by CMB observations.

The amplitude of the correction to the power spectrum is proportional to the energy density during inflation measured in units of the reference mass, which is clearly huge and illustrates the potential of cosmology to test the quantum theory, given that its characteristic scales differ by orders of magnitude from those in the laboratory. The correction is also slow roll suppressed because of the relation between $\delta\rho/\rho$ and ζ [since only the perturbations are quantized, the classical part $\bar{\rho}$ cancels out in Eq. (1)]. This suppression, however, is not sufficient to compensate for the hugeness of $\bar{\rho}_{\mathrm{inf}}/m_0^2$.

In the standard situation, since the power spectrum of ζ is frozen on large scales, its value at the end of inflation is what we observe on the CMB last scattering surface and the calculation can be stopped here. In the CSL theory however, this may no longer be true; hence, one needs to extend the present analysis to the radiation era that follows inflation. During this epoch, the quantities $\alpha_{\boldsymbol{k}}$ and $\beta_{\boldsymbol{k}}$ read

$$\alpha_{\boldsymbol{k}} \equiv \frac{24 M_{\mathrm{Pl}}^2 H^2}{z} e^{-k^2 r_c^2/2a^2} \left[3\left(\frac{aH}{k}\right)^2 - 1\right], \tag{10}$$

$$\beta_{\boldsymbol{k}} \equiv \frac{12 M_{\mathrm{Pl}}^2 H}{az} e^{-k^2 r_c^2/2a^2} \left[1 - 6\left(\frac{aH}{k}\right)^2\right]. \tag{11}$$

The power spectrum of the Mukhanov-Sasaki variable can then be determined using the same techniques as before, and one obtains

$$\mathcal{P}_v(k) = \frac{k^3}{2\pi^2} \frac{1}{4\Re\mathrm{e}\Omega_{\boldsymbol{k}}|_{\gamma=0}} \left[1 + \frac{448}{3}\frac{\gamma}{m_0^2}\bar{\rho}_{\mathrm{end}}\epsilon_1 \left(\frac{k}{aH}\right)^{-1}_{\mathrm{end}} - \frac{\Re\mathrm{e}\Omega_{\boldsymbol{k}}|_{\gamma=0}}{\Re\mathrm{e}\Omega_{\boldsymbol{k}}}\right], \tag{12}$$

where $\bar{\rho}_{\mathrm{end}}$ is the energy density at the end of inflation. Comparing with Eq. (9), one can see that the power spectrum indeed evolves during the transition between inflation and the radiation era, but quickly settles to a constant value, which is therefore the power spectrum probed by CMB experiments. The CSL terms introduce a correction with a spectral index $n_{\mathrm{S}} = 0$. One can also determine the collapse criterion $R = 1152\gamma\bar{\rho}_{\mathrm{end}}(-k\eta_{\mathrm{end}})^{-7}/m_0^2$.

So far, we have assumed that the scale r_c was crossed out during inflation. Let us now examine the situation where r_c is crossed out during the radiation era. In that case, prior to crossing and in particular during the entire inflationary phase, the standard results remain valid. After crossing, the CSL terms become important and, using again the same techniques, one obtains

$$\mathcal{P}_v(k) = \frac{k^3}{2\pi^2} \frac{1}{4\Re\mathrm{e}\Omega_{\boldsymbol{k}}|_{\gamma=0}} \left[1 + \frac{35408}{429}\frac{\gamma}{m_0^2}\bar{\rho}_{\mathrm{end}}\epsilon_1 \times \left(\frac{r_c}{\ell_{\mathrm{H}}}\right)^{-9}_{\mathrm{end}} \left(\frac{k}{aH}\right)^{-10}_{\mathrm{end}} - \frac{\Re\mathrm{e}\Omega_{\boldsymbol{k}}|_{\gamma=0}}{\Re\mathrm{e}\Omega_{\boldsymbol{k}}}\right]. \tag{13}$$

As before, the spectrum is frozen out on super-Hubble scales, but the CSL correction now has spectral index $n_{\mathrm{S}} = -9$. The collapse criterion is given by $R = 7264\gamma/(11 m_0^2)\bar{\rho}_{\mathrm{end}}(k\eta_{\mathrm{end}})^{-14}(H_{\mathrm{end}} r_c)^{-7}$.

Since the CSL corrections are strongly scale dependent, they are ruled out by CMB measurements. Therefore, using that $k/(aH)|_{\mathrm{end}} = e^{-\Delta N}$, where ΔN is the number of e-folds spent by a mode between Hubble radius crossing during inflation and the end of inflation (typically, for scales of cosmological interest today, $\Delta N \sim 50$), one concludes that $\gamma \ll m_0^2(448\bar{\rho}_{\mathrm{end}}\epsilon_1/3)^{-1}e^{-\Delta N}$ if $H_{\mathrm{end}} r_c < e^{\Delta N}$ and $\gamma \ll m_0^2(35408\bar{\rho}_{\mathrm{end}}\epsilon_1/429)^{-1}(H_{\mathrm{end}} r_c)^9 e^{-10\Delta N}$ if $H_{\mathrm{end}} r_c > e^{\Delta N}$. Moreover, the requirements that collapse has occurred when the CMB is emitted, which is equivalent to $R < 1$, leads to $\gamma > m_0^2(1152\bar{\rho}_{\mathrm{end}})^{-1}(-k\eta_{\mathrm{end}})^7$ if $H_{\mathrm{end}} r_c < e^{\Delta N}$ and $\gamma > m_0^2(7264\bar{\rho}_{\mathrm{end}}/11)^{-1}(-k\eta_{\mathrm{end}})^{14}(H_{\mathrm{end}} r_c)^7$ if $H_{\mathrm{end}} r_c > e^{\Delta N}$. These constraints are represented in Fig. 3.

These results allow us to conclude that if the CSL theory is embedded in GR with the Newtonian density contrast, then the parameter values that remain allowed by current laboratory experiments are excluded by CMB measurements. Therefore, that version of CSL is now ruled out.

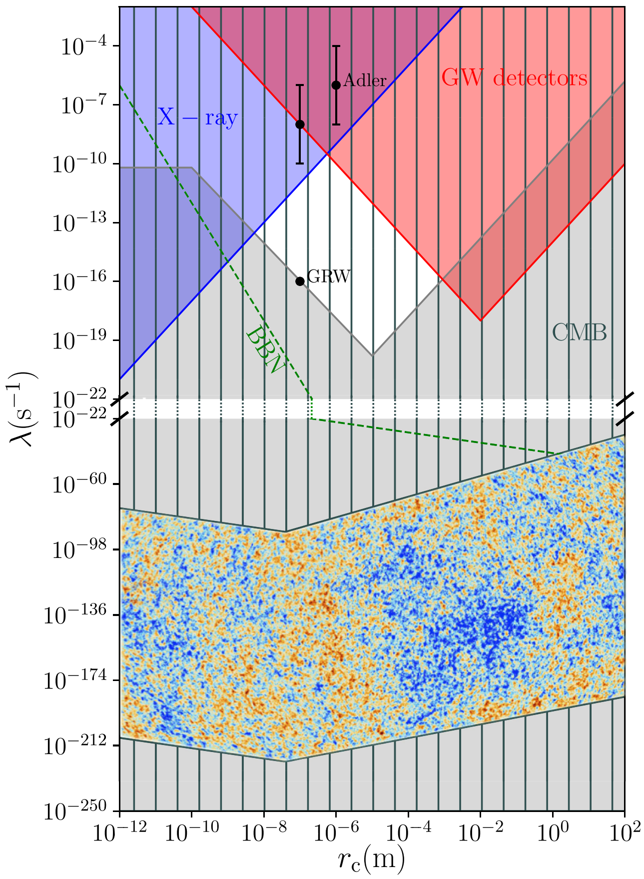

FIG. 3. Observational constraints on the two parameters r_c and λ of the CSL model. The white region is allowed by laboratory experiments, while the unbarred region is allowed by CMB measurements (one uses $\Delta N = 50$ for the pivot scale of the CMB, $H_{\mathrm{inf}} = 10^{-5} M_{\mathrm{Pl}}$ and $\epsilon_1 = 0.005$). The two allowed regions are incompatible. The green dashed line stands for the upper bound on λ if inflation proceeds at the Big-Bang nucleosynthesis (BBN) scale.

As stressed above, other choices for the density contrast could be made. On large scales, they can be generically related to the Newtonian density contrast δ_g by $\delta_p \propto \delta_g [k/(aH)]^p$, where p is a free index. Then, the term $\propto k^{-1}$ in Eq. (12) becomes $\propto k^{2p-1}$, while in Eq. (13), the term $\propto k^{-10}$ becomes $\propto k^{4p-10}$ and the term $\propto (r_c/\ell_H)^{-9}$ becomes $\propto (r_c/\ell_H)^{2p-9}$. This implies that any choice corresponding to $p < 2$ is ruled out. When derived from a more fundamental theory, the CSL model should thus come with a prescription for the density contrast, that crucially conditions the cosmological constraints. However, as explained in the Supplemental Material [57], any “natural” choice for the density contrast leads to $p = 0$, with the one exception of the density contrast denoted δ_m in Ref. [53], which corresponds to $p = 2$. Our result therefore demonstrates that astrophysical data are already accurate enough to rule out CSL theories, except for a small subset of choices for the density contrast.

Further subtleties could also arise if the CSL model was formulated in a field-theoretic manner [4,58–60] (which is in principle required in the present context—although at linear order all Fourier modes decouple and can be treated quantum mechanically), where parameter values may, e.g., run with the energy scale at which the experiment is performed. Other approaches, e.g., Diósi-Penrose model [3,61] where gravity is responsible for the collapse or scenarios where dissipative effects are taken into account [62], could also lead to different results. Other scenarios for forming cosmological structures in the early Universe, such as bouncing cosmologies, could also be investigated.

Despite these uncertainties, the fact that astrophysical data can constrain CSL highlights the usefulness of early Universe observations to discuss foundational issues in quantum mechanics.

V. V. acknowledges funding from the European Union’s Horizon 2020 research and innovation programme under the Marie Skłodowska-Curie Grant No. 750491. It is a pleasure to thank Angelo Bassi for interesting comments and discussions.

*jmartin@iap.fr
†vincent.vennin@apc.in2p3.fr

[1] A. Bassi, K. Lochan, S. Satin, T. P. Singh, and H. Ulbricht, Rev. Mod. Phys. **85**, 471 (2013).
[2] G. C. Ghirardi, A. Rimini, and T. Weber, Phys. Rev. D **34**, 470 (1986).
[3] L. Diosi, Phys. Rev. A **40**, 1165 (1989).
[4] G. C. Ghirardi, P. M. Pearle, and A. Rimini, Phys. Rev. A **42**, 78 (1990).
[5] A. Bassi and G. C. Ghirardi, Phys. Rep. **379**, 257 (2003).
[6] A. Valentini, Phys. Lett. **156A**, 5 (1991).
[7] A. Valentini, Phys. Lett. **158A**, 1 (1991).
[8] C. Curceanu, B. C. Hiesmayr, and K. Piscicchia, J. Adv. Phys. **4**, 263 (2015).
[9] A. Vinante, M. Bahrami, A. Bassi, O. Usenko, G. Wijts, and T. H. Oosterkamp, Phys. Rev. Lett. **116**, 090402 (2016).
[10] M. Carlesso, A. Bassi, P. Falferi, and A. Vinante, Phys. Rev. D **94**, 124036 (2016).
[11] A. Perez, H. Sahlmann, and D. Sudarsky, Classical Quantum Gravity **23**, 2317 (2006).
[12] P. M. Pearle, in *Foundational Questions Institute Inaugural Workshop, FQXi 2007 Reykjavik, Iceland, 2007* (2007) [arXiv:0710.0567].
[13] K. Lochan, S. Das, and A. Bassi, Phys. Rev. D **86**, 065016 (2012).
[14] J. Martin, V. Vennin, and P. Peter, Phys. Rev. D **86**, 103524 (2012).
[15] P. Cañate, P. Pearle, and D. Sudarsky, Phys. Rev. D **87**, 104024 (2013).
[16] M. P. Piccirilli, G. Len, S. J. Landau, M. Benetti, and D. Sudarsky, Int. J. Mod. Phys. D **28**, 1950041 (2019).
[17] G. Leon, A. Majhi, E. Okon, and D. Sudarsky, Phys. Rev. D **98**, 023512 (2018).

[18] G. Leon, A. Pujol, S. J. Landau, and M. P. Piccirilli, Phys. Dark Universe **24**, 100285 (2019).
[19] N. Pinto-Neto, G. Santos, and W. Struyve, Phys. Rev. D **85**, 083506 (2012).
[20] J. Martin and V. Vennin, Phys. Rev. D **93**, 023505 (2016).
[21] J. Martin and V. Vennin, Phys. Rev. D **96**, 063501 (2017).
[22] R. de Putter and O. Doré, arXiv:1905.01394.
[23] D. Sudarsky, Int. J. Mod. Phys. D **20**, 509 (2011).
[24] J. von Neumann, *Mathematical Foundations of Quantum Mechanics* (Princeton University Press, Princeton, 1955).
[25] J. B. Hartle, arXiv:1901.03933.
[26] D. Polarski and A. A. Starobinsky, Classical Quantum Gravity **13**, 377 (1996).
[27] A. Albrecht, P. Ferreira, M. Joyce, and T. Prokopec, Phys. Rev. D **50**, 4807 (1994).
[28] A. A. Starobinsky, Phys. Lett. **91B**, 99 (1980).
[29] A. H. Guth, Phys. Rev. D **23**, 347 (1981).
[30] A. D. Linde, Phys. Lett. **108B**, 389 (1982).
[31] A. Albrecht and P. J. Steinhardt, Phys. Rev. Lett. **48**, 1220 (1982).
[32] A. D. Linde, Phys. Lett. **129B**, 177 (1983).
[33] J. Martin and C. Ringeval, J. Cosmol. Astropart. Phys. 08 (2006) 009.
[34] L. Lorenz, J. Martin, and C. Ringeval, J. Cosmol. Astropart. Phys. 04 (2008) 001.
[35] L. Lorenz, J. Martin, and C. Ringeval, Phys. Rev. D **78**, 063543 (2008).
[36] J. Martin, C. Ringeval, and R. Trotta, Phys. Rev. D **83**, 063524 (2011).
[37] J. Martin and C. Ringeval, Phys. Rev. D **82**, 023511 (2010).
[38] J. Martin, C. Ringeval, and V. Vennin, Phys. Dark Universe **5–6**, 75 (2014).
[39] J. Martin, C. Ringeval, R. Trotta, and V. Vennin, J. Cosmol. Astropart. Phys. 03 (2014) 039.
[40] J. Martin, C. Ringeval, and V. Vennin, Phys. Rev. Lett. **114**, 081303 (2015).
[41] J. Martin, arXiv:1502.05733.
[42] V. F. Mukhanov and G. Chibisov, JETP Lett. **33**, 532 (1981).
[43] Y. Akrami *et al.* (Planck Collaboration), arXiv:1807.06205.
[44] Y. Akrami *et al.* (Planck Collaboration), arXiv:1807.06211.
[45] H. Kodama and M. Sasaki, Prog. Theor. Phys. Suppl. **78**, 1 (1984).
[46] D. J. Schwarz, C. A. Terrero-Escalante, and A. A. Garcia, Phys. Lett. B **517**, 243 (2001).
[47] S. M. Leach, A. R. Liddle, J. Martin, and D. J. Schwarz, Phys. Rev. D **66**, 023515 (2002).
[48] J. Martin and V. Vennin, arXiv:1912.07429.
[49] J. S. Schwinger, Phys. Rev. **82**, 664 (1951).
[50] V. V. Dodonov, Phys. Scr. **82**, 038105 (2010).
[51] W. G. Unruh, Phys. Rev. D **14**, 870 (1976).
[52] S. W. Hawking, Commun. Math. Phys. **43**, 199 (1975).
[53] J. M. Bardeen, Phys. Rev. D **22**, 1882 (1980).
[54] T. Bunch and P. Davies, Proc. R. Soc. A **360**, 117 (1978).
[55] G. Lindblad, Commun. Math. Phys. **48**, 119 (1976).
[56] J. Martin and V. Vennin, J. Cosmol. Astropart. Phys. 05 (2018) 063.
[57] See Supplemental Material at http://link.aps.org/supplemental/10.1103/PhysRevLett.124.080402 for more technical details.
[58] R. Tumulka, Proc. R. Soc. A **462**, 1897 (2006).
[59] D. J. Bedingham, Found. Phys. **41**, 686 (2011).
[60] D. Bedingham, D. Dürr, G. Ghirardi, S. Goldstein, R. Tumulka, and N. Zanghì, J. Stat. Phys. **154**, 623 (2014).
[61] R. Penrose, Gen. Relativ. Gravit. **28**, 581 (1996).
[62] A. Smirne and A. Bassi, Sci. Rep. **5**, 12518 (2015).